IEEE Access
Multidisciplinary ⋮ Rapid Review ⋮ Open Access Journal

Received 20 March 2024, accepted 6 April 2024, date of publication 11 April 2024, date of current version 22 April 2024.

Digital Object Identifier 10.1109/ACCESS.2024.3387565

RESEARCH ARTICLE

Efficient Numerical Synthesis of Radiation Patterns Using Circuit Model for Substrate Integrated Waveguide Leaky Wave Antennas

NASIM ZAHRA[1], FAROOQ MUKHTAR[1], INAM ELAHI RANA[2], AND MAHRUKH KHAN[3]
[1]Department of Electrical Engineering, University of Engineering and Technology Lahore, Lahore 54890, Pakistan
[2]Bismillah Electronics, Lahore 54600, Pakistan
[3]Electrical and Computer Engineering Department, The College of New Jersey, Ewing, NJ 08628, USA

Corresponding author: Nasim Zahra (nasimzahra132@hotmail.com)

ABSTRACT A novel approach is presented for synthesizing radiation patterns of substrate-integrated waveguide leaky wave antennas in two stages. In the first stage, the antenna is considered an equivalent rectangular waveguide with slots, and a comprehensive equivalent circuit model is constructed. Varying slot configurations are accommodated by the developed equivalent circuit model. Each slot section is represented as an admittance with the incorporation of Elliott's slot theory. Computations of the relative aperture fields are performed using circuit theory, and the far-field pattern is estimated through array theory. In the second stage, the circuit model is utilized for genetic algorithm-based optimization, enabling customization of the radiation pattern to meet specific requirements. The methodology has a computational advantage over full-wave simulations, resulting in a significantly faster and more efficient design process. Numerical verification through simulation of various examples and experimental validation through antenna fabrication are presented, affirming agreement between calculated and measured results. Remarkable effectiveness in antenna engineering can be attained for future wireless communication systems by using the proposed technique.

INDEX TERMS Leaky wave antenna, modeling of antenna, optimization, pattern synthesis, substrate integrated waveguide.

I. INTRODUCTION

A substrate-integrated waveguide (SIW) is a dielectric-filled parallel plate waveguide with two rows of metallic cylinders within which electromagnetic waves are confined [1]. The waveguide technique is used to integrate a rectangular waveguide into a dielectric substrate. Its applications, including antennas, filters, multiplexers, couplers, and power dividers, all benefit from their low loss, cost-effective manufacturing, and seamless integration with planar circuits, in contrast to traditional bulky waveguides.

Leaky wave antennas (LWAs) are generally developed based on various transmission lines or waveguides integrated with radiating discontinuities (RDs) [2], [3], [4], [5], [6], [7], [8], [9], [10], [11]. The inclusion of RDs or perturbations is essential for transforming nonradiating guides into open and radiative structures. Consequently, the loading effects of RDs, particularly their impedance and admittance properties, inevitably affect the operating leaky mode of LWAs in terms of the associated attenuation and phase constants [7], [8], [9], [10], [11], [12], [13], [14]. An intriguing utilization of SIW is found to be LWA [15], where energy radiation is enabled by large periodic gaps between vias. Extensive exploration of SIW-based LWAs is undertaken in [15], [16], [17], and [18], driven by their inherent ability to scan with frequency. This attribute renders them appealing for 5G base station antennas, providing scalability, cost efficiency, and straightforward feed design [9].

The associate editor coordinating the review of this manuscript and approving it for publication was Fulvio Schettino.

Researchers have proposed various techniques for modeling and generating far-field patterns for SIW LWAs [3], [4], [5], [6]. In [3], the SIW LWA is modeled as a Transverse Equivalent Network (TEN). The focus has been on SIW LWA design, with specific beamwidth and scanning angle parameters achieved through the control of the waveguide width and period of the vias. Nevertheless, it is constrained to periodic structures and does not consider sidelobe levels (SLL) or other pattern parameters. In an alternative approach [4], the antenna is presented as a lossy transmission line, divided into sections as two-port networks. Although effective for certain LWAs, it encounters problems with accuracy in the presence of rapid profile variations. The concepts introduced in [19], [20], and [21] are generalized by [4]. In the latest work, a nonconventional array theory approach is applied to design an SIW LWA [5]. This approach is based on the general principle of pattern multiplication using the phase of the antenna element [22]. Both the element pattern and array factor exhibit a frequency dependence. Wide scanning is achieved, though there is no explicit way to control side lobe levels (SLLs) or other performance parameters. A simulation model is introduced in [6], refining far-field patterns through the adjustment of slot dimensions and associated amplitude weighting for a slotted waveguide structure on SIW technology. Gain can be maximized for the optimum number of slots, while balancing performance parameters. Low SLLs can be achieved by choosing appropriate weighting coefficients.

This study introduces a novel transmission-line-based circuit model for SIW LWAs. By considering large openings between vias as slots and integrating them into a circuit model as shunt loading, the distributions of the aperture fields across these slots are determined by solving the circuit. Array theory is then applied to these fields to derive far-field radiation patterns. This approach incorporates optimization techniques to minimize differences between the desired radiation pattern (encompassing scanning angle $\theta_{Desired}$ and beamwidth) and the calculated pattern.

Compared with previous approaches [3], [4], this work offers a more versatile methodology for pattern synthesis in both periodic and quasi-periodic structures. Effective minimization of the SLL and consideration of diverse pattern parameters are possible. In line with [5], the element pattern is predetermined, and the phase of the array factor is manipulated. This is done by adjusting slot openings, changing the spacing between slots, and varying their numbers. In a manner akin to [6], weighting coefficients in the array factor are adjusted through an optimization process to achieve the desired pattern. In this context, these weighting coefficients correspond to the voltages across slot admittances in the circuit. The implementation of phase manipulation and the determination of coefficients in the array factor rely on the proposed circuit model. Furthermore, this circuit-centric approach exhibits cost-efficient computational performance compared to traditional full-wave simulation-based software, aided by the utilization of optimization techniques, such as genetic algorithms in MATLAB, facilitating the efficient identification of optimal solutions within predefined constraints. A circuit model can be used for initial design exploration and optimization, followed by detailed electromagnetic simulations to validate and fine-tune the design. This work provides a tool for designing SIW LWAs with radiation patterns and scanning angles of reasonable accuracy. Its potential for advancing antenna engineering in 5G communication is underscored by its flexibility, accuracy, scalability, and computational efficiency.

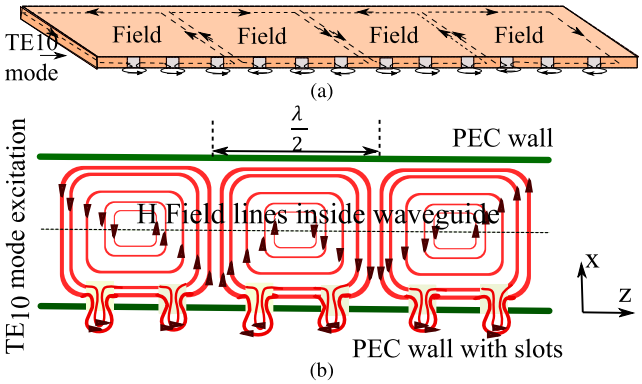

FIGURE 1. Equivalent rectangular waveguide for SIW LWA with slots in its narrow wall (a) TE_{10} mode H-field making round through slots (Oblique view) (b) Top view of a slot-based waveguide with H-field lines inside the waveguide section.

Section II provides insight that, regardless of the size of the slot, the field distribution on the slot aperture approximates a half sine wave. The peaks and phases of these sine waves vary from slot to slot due to the leaky nature of the antenna. Aperture fields of the same shape result in corresponding far-field patterns of the same shape. Superposition is applied to determine the overall radiation pattern for an array of slots. The slot section model as shunt admittance, detailed theory for circuit modeling, and formulation of cost function for optimization are presented in section III. Simulation results for different examples are presented in section IV for numerical verification and in section V, measured results are displayed for experimental validation. Detailed comparison with other models can be found in Table 1 of section V.

II. SIW LEAKY WAVE ANTENNA

SIW becomes a leaky wave antenna if the spacing between its vias is adequate [15]. A simplified diagram of the equivalent rectangular waveguide of SIW LWA is shown in Fig. 1, obtained using equivalent width formulae given in [16]. All walls serve as conducting planes except large gaps between vias are substituted with rectangular slots having the same height as the substrate thickness. When this waveguide is excited by the TE_{10} mode, H-field lines of the mode

experience disturbance in the vicinity of the slots, as depicted in Fig. 1. Slot apertures can act as magnetic dipoles for very small openings and can be considered as an array of magnetic dipoles.

Wide slots in the waveguide structure act as radiation sources, perturbing the mode field within and introducing extra leaky attenuation and phase changes. This causes a significant field spread outside the waveguide, as shown in Fig. 2. Specifically, the E_y component of the mode field exhibits an intuitively observed half-sine wave shape, where it has a nonzero value at the slot's center and smoothly diminishes to zero at the edges, a behavior stemming from the perfect electric boundary characteristics of the surrounding wall, as depicted in Fig. 3. The radiation patterns of slots with similar tangential field shapes share the same overall shape, differing mainly in peak values and phases. Superposition can be employed to determine the radiation pattern produced by an array of these slots, considering relative aperture field changes. This technique is versatile and can be applied to a range of waveguide structures with slots, utilizing either general array theory or the equivalence principle, while considering their specific constraints and limitations.

III. RADIATION PATTERN RADIATED FROM SIW LWA

A. DETERMINATION OF ADMITTANCE (Y) FOR A SLOT SECTION

A radiating discontinuity in a waveguide structure can be described using either series or shunt-loading models [2]. Slots on a substrate-integrated waveguide structure are modeled as impedances in [7] and [8], and as admittances in [12] and [13] by manipulating the equivalent magnetic surface currents. Elliott's slot theory in [11] models a resonant slot on a waveguide structure as a shunt conductance in a transmission line (TL). Rectangular waveguide-based LWAs with hole-shaped slots are modeled as a complex shunt impedance by Oliner and Goldstone [10]. Here in this work, the slot is not in a resonant state. Consequently, the admittance presented in the TL model is complex. Irrespective of the slot shape and structure of the waveguide section, by using S-parameters data generated by full-wave simulation or even by measurement, Y can be derived for any unit slot waveguide section.

Consider a section of a waveguide containing a single aperture, as shown in Fig. 4(a). A symmetrical waveguide section of length L and cross-sectional dimensions a and b, containing a slot of length s in the middle, is taken and shown in Fig. 4(a). An equivalent circuit model for this waveguide section is exhibited in Fig. 4(b). Length $L/2$ is taken from the middle of the slot to either side of the waveguide section. The waveguide is depicted as a TL with impedance Z_w and propagation constant γ, where these parameters are calculated for the TE_{10} mode. The slot section is modeled as a complex admittance, where $Y = G + jB$. G is proportional to radiation loss, and B is responsible for phase change [14]. It is characterized by the parameters: length s, width b, dielectric material with permittivity ϵ, and frequency of operation f. The ABCD matrix is calculated for the unit slot waveguide section, and is given in (1).

$$\begin{bmatrix} \cosh\gamma L/2 & Z_w \sinh\gamma L/2 \\ \frac{\sinh\gamma L/2}{Z_w} & \cosh\gamma L/2 \end{bmatrix} \times \begin{bmatrix} 1 & 0 \\ Y & 1 \end{bmatrix} \times \begin{bmatrix} \cosh\gamma L/2 & Z_w \sinh\gamma L/2 \\ \frac{\sinh\gamma L/2}{Z_w} & \cosh\gamma L/2 \end{bmatrix} = \begin{bmatrix} A & B \\ C & D \end{bmatrix} \tag{1}$$

where,

$$\begin{aligned} A &= \frac{Z_w Y \sinh\gamma L}{2} + \cosh\gamma L, \\ B &= Z_w \sinh\gamma L + \frac{Z_w^2\, Y \cosh\gamma L}{2} - \frac{Z_w^2\, Y}{2}, \\ C &= \frac{\sinh\gamma L}{Z_w} + \frac{Y \cosh\gamma L}{2} + \frac{Y}{2}, \\ D &= \cosh\gamma L + \frac{Z_w Y \sinh\gamma L}{2}. \end{aligned}$$

Using conversion formulae available in [23], S-parameters can be obtained from ABCD parameters. The Y can be calculated from S-parameters, as given in (2).

$$Y = \frac{(2\cosh\gamma L + Q\sinh\gamma L)\, S_{11} - R\sinh\gamma L}{\frac{Z_w}{2}\left[R\cosh\gamma L - Q - (Q\cosh\gamma L + 2\sinh\gamma L - R)\, S_{11}\right]} \tag{2a}$$

$$Y = \frac{2 - S_{21}(2\cosh\gamma L + Q\sinh\gamma L)}{S_{21}\frac{Z_w}{2}(Q\cosh\gamma L + 2\sinh\gamma L - R)} \tag{2b}$$

where, $Q = \left[\frac{Z_w}{Z_0} + \frac{Z_0}{Z_w}\right]$, $R = \left[\frac{Z_w}{Z_0} - \frac{Z_0}{Z_w}\right]$

The variation in Y value of a slot section depends on the frequency, structural design parameters, S-parameters, γ, and impedances, as mentioned in (2). S-parameters, γ, and impedances themselves depend on frequency. In addition to frequency, S-parameters vary with port impedance Z_0 and waveguide impedance Z_w. Here, Z_w represents the impedance at any arbitrary operating frequency, whereas Z_0 signifies the port impedance at a specific frequency.

B. DETERMINATION OF SLOT APERTURE FIELDS

To obtain radiation patterns for slots-based leaky wave antennas, it is necessary to know the relative magnitudes and phases of tangential electric fields for these slots. These fields are directly proportional to the corresponding voltages of admittances in the equivalent circuit model, for which analytical expressions are derived below.

A waveguide with n number of slots is shown in Fig. 5(a), and the circuit model is presented in Fig. 5(b), where each slot section is depicted as a shunt admittance. There will be $n+1$ sections of the waveguide for n number of slots. Four steps are involved in determining the aperture voltages of n number of slots. First, the ABCD matrix for any m^{th} section

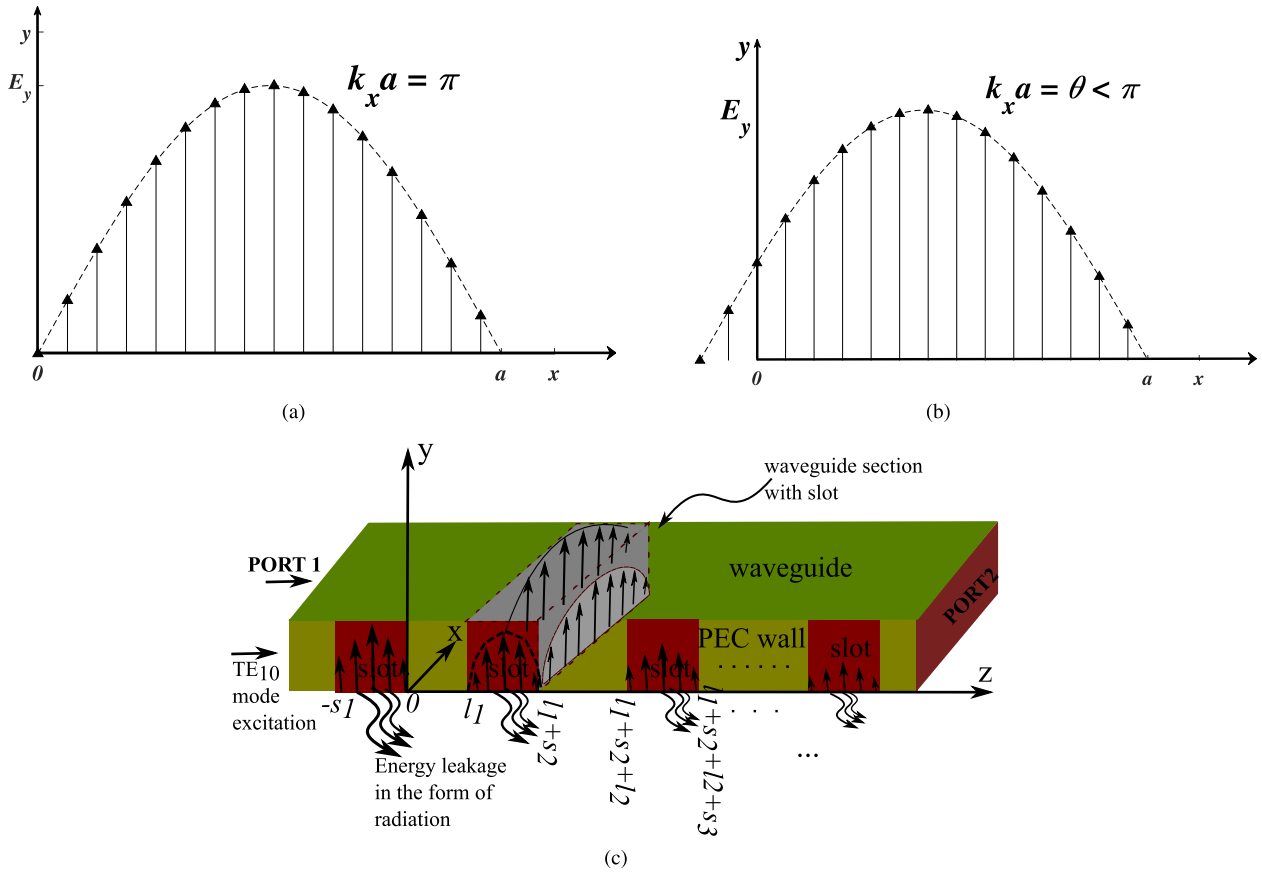

FIGURE 2. SIW LWA equivalent rectangular waveguide with slots in its narrow wall. (a) Mode Field at the edges of the slot. (b) Mode field at the center of the slot. (c) Depiction of perturbed TE_{10} field due to leaky nature of the antenna because of slots.

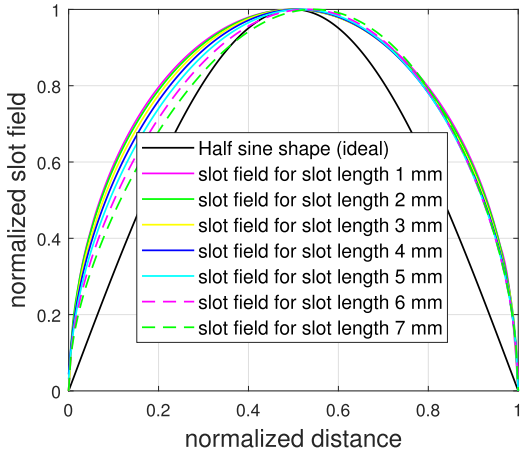

FIGURE 3. Electric field on slot aperture for different slot opening lengths at 15 GHz.

of the waveguide will be calculated, as given in (3):

$$\begin{bmatrix} A_m & B_m \\ C_m & D_m \end{bmatrix} = \begin{bmatrix} \cosh \gamma L_m & Z_w \sinh \gamma L_m \\ \frac{\sinh \gamma L_m/2}{Z_w} & \cosh \gamma L_m \end{bmatrix} \tag{3}$$

Second, the impedance looking into any m^{th} section and towards the load side will be calculated, as given in (4):

$$Z_{in,m} = Z_0 \left(\frac{\frac{1}{Y_m^{/}} + Z_0 \tanh \gamma L_m}{Z_0 + \frac{1}{Y_m^{/}} \tanh \gamma L_m} \right) \tag{4}$$

Equations (3) and (4) can be modified for lossless cases by ignoring the attenuation constant in γ and using standard identities of hyperbolic functions. Third, the calculated impedances from (4) will be used to calculate equivalent admittances looking into the m^{th} section of the waveguide and from the source side in parallel with the n^{th} slot admittance, as given in (5):

$$Y_n^{/} = Y_n + \frac{1}{Z_{in,m}} \tag{5}$$

Here, $m = n + 1$.

Where Y_n is the value of admittance of n^{th} slot section that can be found by using (2). Fourth, admittances from (5) and ABCD parameters from (3) will be used to find excitation voltage for each n^{th} slot, as shown in (6).

$$V_n = \left[\frac{1}{A_n + B_n Y_n^{/}} \right] V_{n-1} \tag{6}$$

C. DETERMINATION OF RADIATION PATTERN

Radiation patterns can be found using array theory [24]. Element patterns can be generated through full-wave analysis of unit slot waveguide section and circuit analysis would give relative aperture excitation coefficients to calculate array factor (AF). The radiation pattern can be calculated then using element pattern and array factor. For applying array

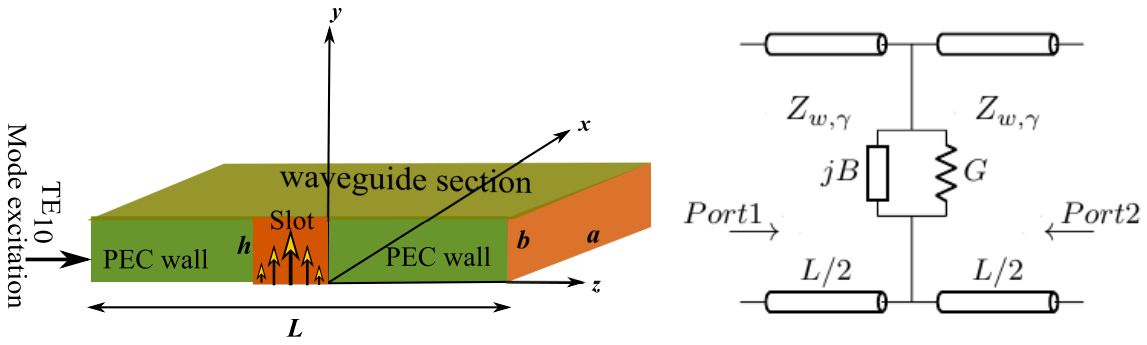

FIGURE 4. Unit slot waveguide section (a) Equivalent rectangular waveguide for SIW, where the perfect electric conducting(PEC) walls can be realized by via-holes with accurate width conversion formula. (b) Equivalent circuit model.

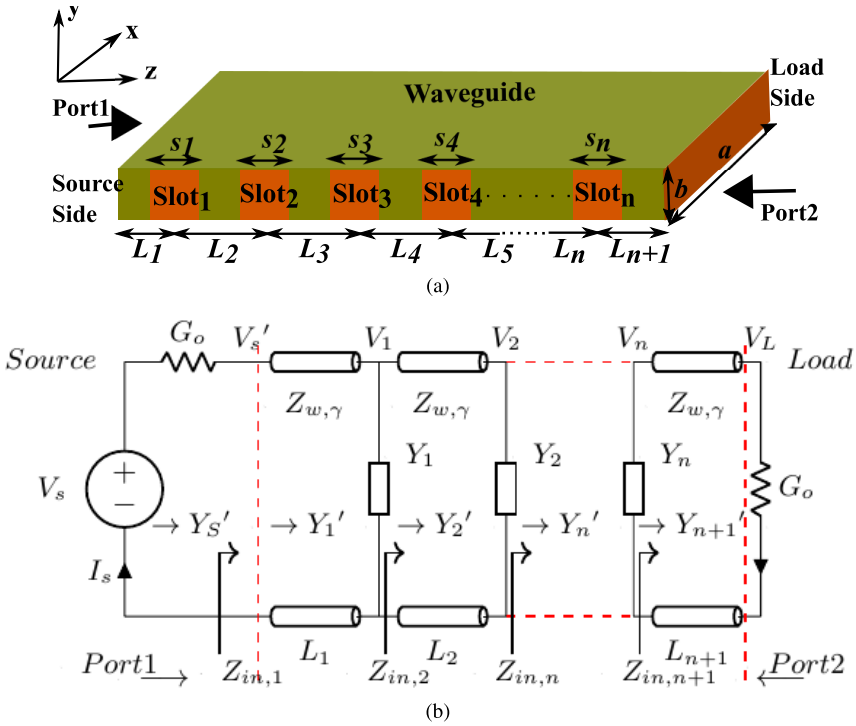

FIGURE 5. *n* number of slots-based LWA (a) Waveguide model (b) Equivalent circuit model.

theory for more than one slot, the factors that can affect the radiation pattern of the waveguide, are the number of slots n, edge-to-edge spacing between slots [$l_1, l_2, l_3, \ldots l_{n-1}$], and opening of slots [$s_1, s_2, \ldots s_n$], referring to Fig. 2(c). The comparison of array theory (AT) generated pattern and full wave simulation generated pattern would verify the accuracy of the proposed circuit model.

D. OPTIMIZATION AND DESIGN CONSIDERATIONS

Optimization plays a major role in finding the best feasible solution when there are constraints and there are so many solutions available. It is done using a genetic algorithm (GA) implemented in MATLAB. Fitness functions and constraints can be devised according to certain applications for which the design goals could be to achieve certain steering angles, beamwidth, gain, wide nulls, and side lobe levels (SLLs).

In generalized waveguide-fed slot antennas, design parameters are number of slots, spacing between slots, and dimension of slots. Other parameters like frequency of operation, the thickness of the substrate, and cross-sectional dimensions of the waveguide are dictated by design requirements and manufacturing constraints.

The design problem can be formulated as an optimization problem by defining an error function as an objective function. The error function is expressed here as a weighted sum of the differences between the desired pattern and the calculated pattern, as shown in (7):

$$\mathrm{OF}(X) = \sum_{\theta} |\mathrm{err}(X, \theta)| \tag{7}$$

where,

$$\mathrm{err}(X, \theta) = \Xi(\theta) - \aleph(X, \theta) \tag{8}$$

Ξ is the specific desired pattern mask. $\aleph$ is the calculated pattern at each iteration of the optimization process. X is the vector of optimization variables; vector $[l_1, l_2, l_3, \ldots . l_{n-1}]$ as P containing edge-to-edge spacing between slots and n variable as total number of slots. The optimization problem can be described as follows in (9),

$$\begin{aligned} \min_{X} \quad & \text{OF}(X) \\ \text{s.t.} \quad & \text{lb} \leq P \leq \text{ub} \\ & \Delta\theta \leq \text{FNBW} \\ & n_1 \leq n \leq n_2 \end{aligned} \tag{9}$$

lb is the lower bound and ub is the upper bound for each entry of P vector in (9). Also, the number of slots is indicated by n with lower and upper limits as n_1 and n_2 respectively.

There are several possibilities to define Ξ. These include shaping the beam, minimizing SLL, maximizing gain in a certain direction, or even a combination of more than one objective function with corresponding specific weights, among many other possibilities, using the proposed circuit model and theoretical expressions. Suppose a beam is required of some beamwidth ($\Delta\theta = \theta_{FN2}$ - θ_{FN1}) with peak directed at $\theta_{Desired}$, where $\Delta\theta$ is the beamwidth of antenna which should be equal to or less than first null beamwidth defined. The expression for Ξ can be written mathematically in (10).

$$\Xi(\theta) = \begin{cases} \text{sinc}\left(\dfrac{2\,(\theta - \theta_{Desired})}{(\theta_{FN2} - \theta_{FN1})}\right) & \theta > \theta_{FN1},\ \theta < \theta_{FN2} \\ 0 & \theta \leq \theta_{FN1},\ \theta \geq \theta_{FN2} \end{cases} \tag{10}$$

In the first expression of (10), $\theta_{Desired} = \underset{\theta}{\arg\max} \mid \text{AF}(\theta) \mid$, where $\theta \in [\theta_{FN1}, \theta_{FN2}]$. AF represents the array factor of the antenna. θ_{FN1} and θ_{FN2} are the first nulls of the main lobe, defining the first null beamwidth (FNBW) of the beam pattern. In the second expression of (10), $\theta \in S$, where $S = [0, \theta_{FN1}] \cup [\theta_{FN2}, \pi]$. S corresponds to the theta space containing side lobe levels, which are implicitly constrained in (10) to be at the minimum level possible. However, achieving exactly zero SLL is not feasible due to antenna structure. SLL below -10 dB is reasonable to be accepted though. It is noted that $0° < \theta < 90°$ in the elevation plane can be optimized to get desired θ by exciting port1, and for $90° < \theta < 180°$, optimization can be achieved by exciting port2.

Circuit model-based optimization on a numeric computing platform is much faster than full wave simulation-based optimization. In the proposed work, the optimization process is performed on theoretically obtained expression for radiation pattern and is compared with the desired pattern at each iteration of the optimization process. The antenna is simulated also on a full wave simulator for optimized vector X. Three patterns; the desired or targeted one, the pattern from full-wave simulation, and the one from the calculation on MATLAB using the circuit model, are then compared in the next section.

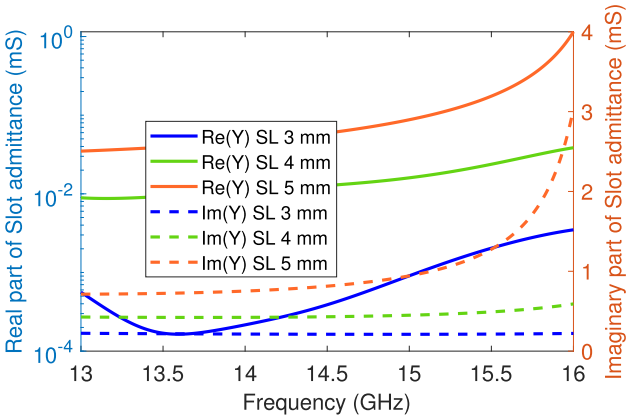

FIGURE 6. Real and imaginary values of admittance of slot section of length (SL) for $\epsilon_r = 2.2$, $tan\delta = 0.0009$, $a = 12.5$ mm, and $b = 1.575$ mm at various frequencies.

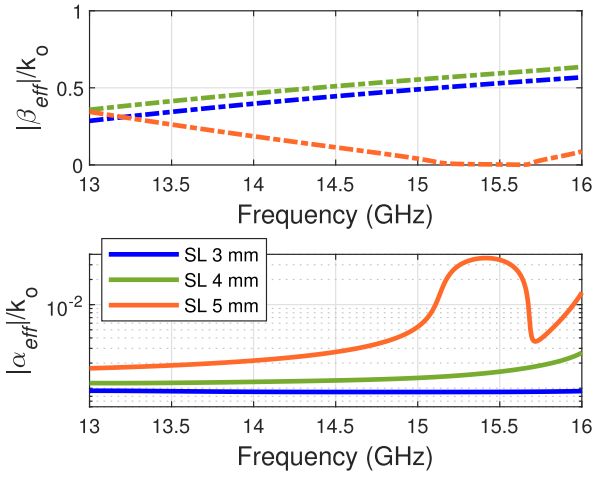

FIGURE 7. The dispersion curves of the unit slot waveguide section for $\epsilon_r = 2.2$, $tan\delta = 0.0009$, $a = 12.5$ mm, and $b = 1.575$ mm.

IV. SIMULATION RESULTS

A. ADMITTANCE OF A SLOT SECTION

Shunt admittance can be calculated by using (2), if S-parameters are available. Required S-parameters data can be obtained by simulating unit slot waveguide section on a full wave simulator or by measurement. Calculated real and imaginary values for admittance are shown in Fig. 6 using full-wave simulation for unit slot waveguide section of particular dimensions and dielectric, as an example. Values vary with slot length and frequency of operation, whereas the dimensions of the waveguide and dielectric with which it is filled are kept constant. The attenuation constant of the leaky mode is related to the real part of the admittance, whereas the phase constant is influenced by the imaginary part of that parameter [14]. It should be noted that the calculated radiation pattern is found to be sensitive to the numerical accuracy of admittance.

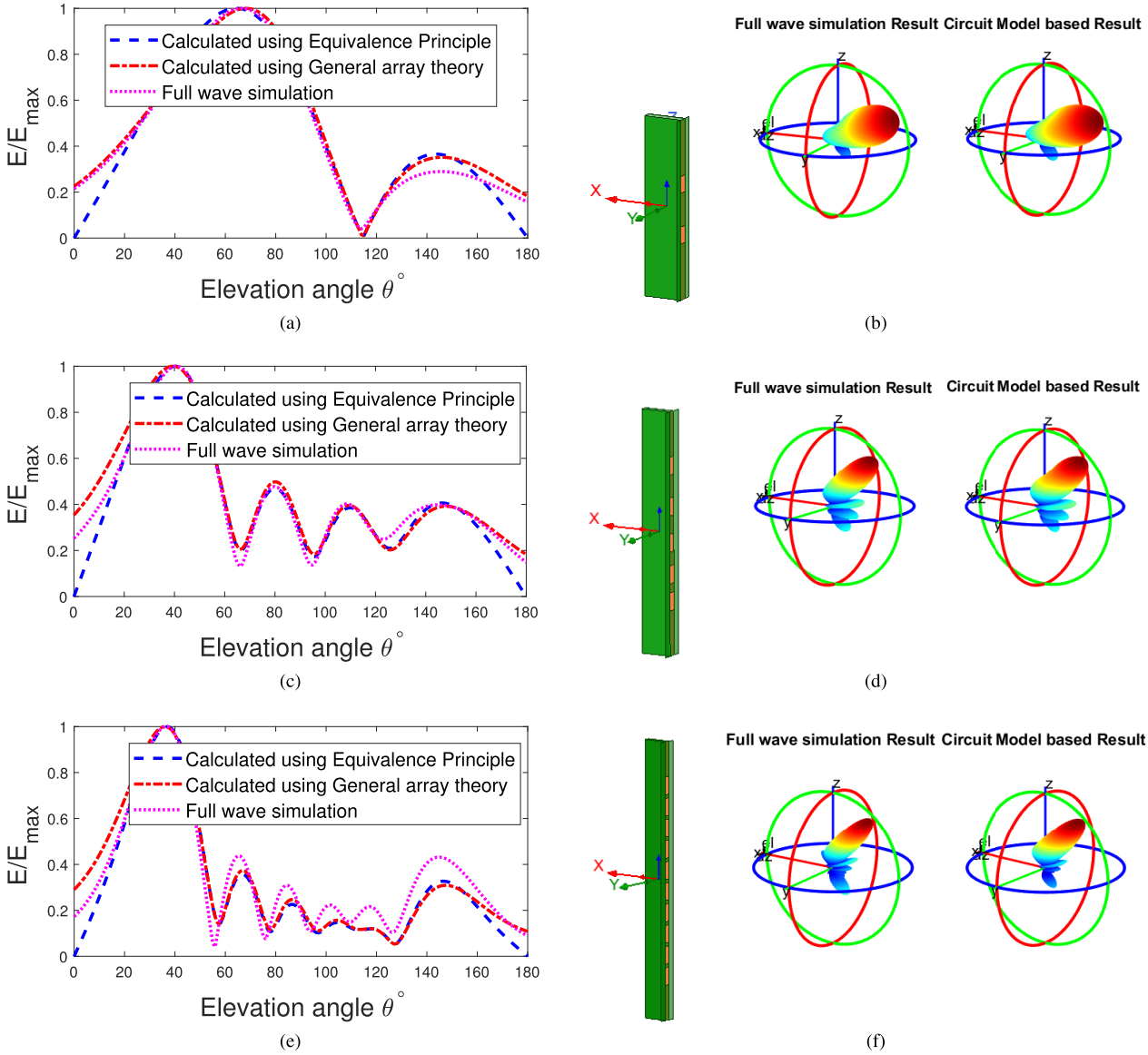

FIGURE 8. Numerical verification (a) Numerical example#1: Radiation pattern in elevation plane at 15 GHz for two 3 mm slots with 6 mm spacing (b) 3D patterns for numerical Example#1 (c) Numerical example#2: Radiation pattern in elevation plane at 16.5 GHz for five 4 mm slots with *P* as [2 3 4 5] in mm (d) 3D patterns for numerical example#2 (e) Numerical example#3: Radiation pattern in elevation plane at 15 GHz for ten 5 mm slots with 1 mm spacing each (f) 3D patterns for numerical example#3.

The effective phase constant (β_{eff}) and attenuation constant (α_{eff}) can be obtained from S-parameters [8], and their representation is shown in Fig. 7 for a particular waveguide dimension and varying slot dimensions. The k_0 represents the wavenumber of free space. In cases where $|\beta_{eff}| < k_0$, electromagnetic waves operate within the fast wave regime, indicating the potential for radiation from the LWA. Radiation is not feasible otherwise. It can be observed that $|\beta_{eff}| < k_0$. The small value of α_{eff} facilitates controlled leakage of energy along the length of the antenna, allowing for radiation.

B. NUMERICAL VERIFICATION OF THE CIRCUIT MODEL

The accuracy of the circuit model is verified in this section. The slot section is simulated on a full wave simulator for extraction of S-parameters and element patterns. The height of the PEC wall is extended in y direction in Fig. 4; above and below the slot to determine the radiation pattern of waveguide with more than one slot using the equivalence principle along with general array theory. A waveguide with more than one slot is realized by replicating a unit slot waveguide structure. Voltages are calculated using the proposed circuit model for the determination of radiation patterns. Both theories will give comparable results in this case. Unit slot waveguide section of dimensions $a = 7$ mm and $b = 1.575$ mm filled with a dielectric of $\epsilon_r = 2.2$ and $\tan\delta = 0.0009$ is used for the examples below. The 2D patterns presented in the elevation plane showcase how well these patterns align at their peak values. Additionally, by displaying 3D patterns, it can be inferred that reasonable similarities extend to their three-dimensional shapes. It should be noted that circuit

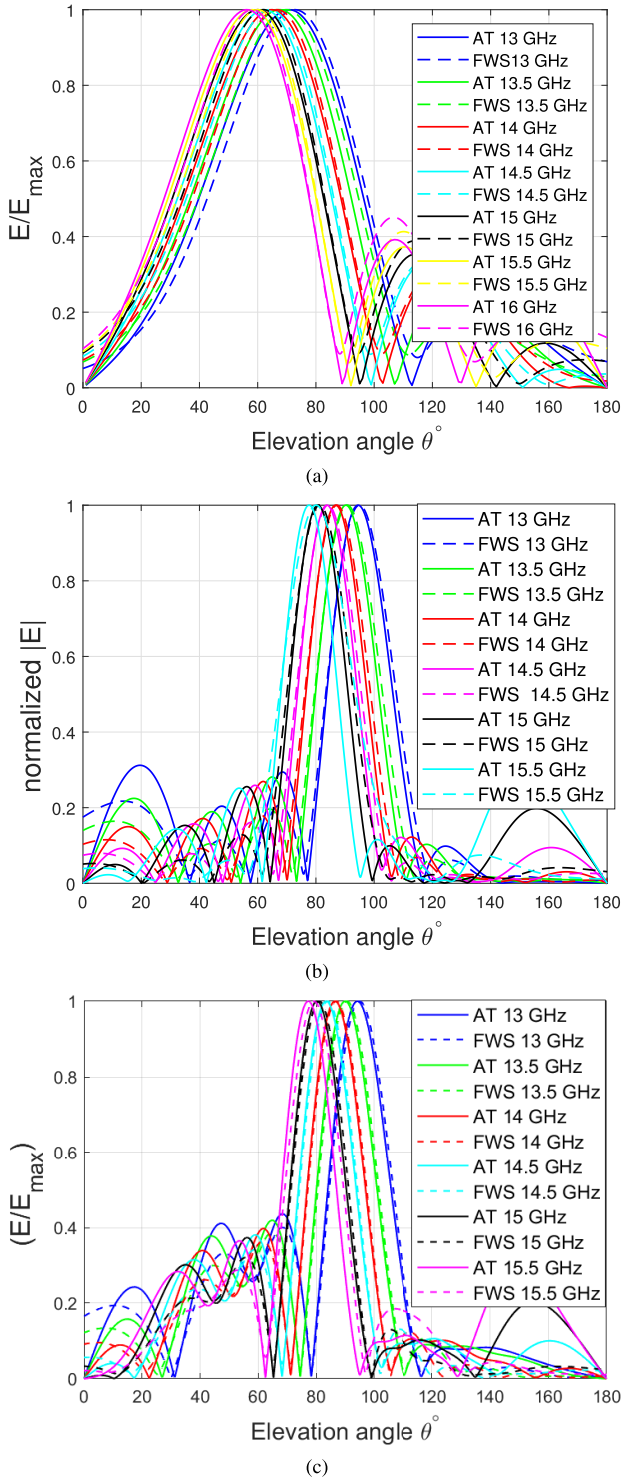

FIGURE 9. Scanning of the radiation pattern with a change in frequency, when $a = 12.5$ mm, $b = 1.575$ mm, $f_o = 15$ GHz (a) Numerical eample#4: $\epsilon_r = 1$, $\tan\delta = 0$, $n = 3$, $s = 2$ mm, $P = [7.57$ mm, 7.47 mm] (b) Numerical eample#5: $\epsilon_r = 2.2$, $\tan\delta = 0.0009$, $n = 8$, $s = 3$ mm, $P = [2.18, 1.00, 3.18, 5.68, 3.05, 1.00, 2.11]$ mm (c) Numerical eample#6: $\epsilon_r = 2.2$, $\tan\delta = 0.0009$, $n = 10$, $s = 3$ mm, $P = [2.47, 7.99, 1.00, 1.00, 7.99, 2.47, 7.99, 1.00, 1.00]$ mm.

model-based 3D patterns displayed in Fig. 8 are calculated using general array theory, which will be used for any type of waveguide structure later.

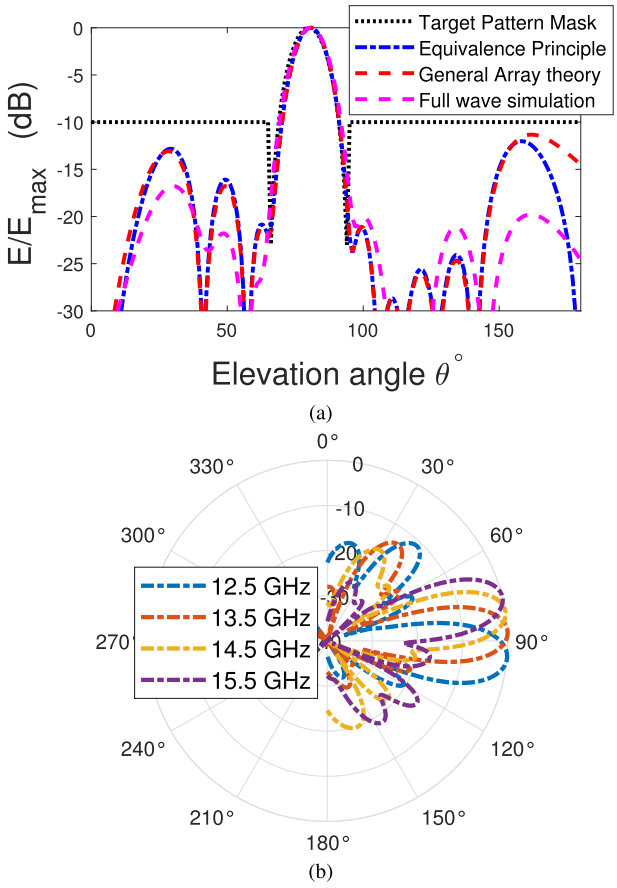

FIGURE 10. Optimized results in elevation plane for design example#1 (a) Normalized radiation pattern at frequency 14.5 GHz (b) Simulated normalized directivity plots showing frequency scanning behavior.

Simulation techniques are frequently utilized to assess various scenarios, including the examination of pattern scanning by changing frequency with the adjustment of admittance values. The simulated results, obtained through full-wave simulation(FWS), closely match the calculated outcomes derived from MATLAB using array theory and circuit model equations, which are referred to as array theory(AT) results and are shown in Fig. 9. This tells that the circuit model accurately represents the behavior of the system, even when considering the changing impedance values with change in frequency.

C. OPTIMIZATION EVALUATION

This section showcases two design examples that demonstrate the optimization process based on the proposed circuit model. The optimization is performed using a genetic algorithm implemented in MATLAB with a population of 200 in each of the 200 generations. The design parameters, P and n, are obtained through cost function optimization. The resulting radiation patterns are compared for both array theory (AT) generated and full wave simulated patterns. The P vector and n are part of the X vector and have to be optimized. The slot openings $[s_1, s_2, \ldots s_n]$ are defined before performing optimization and are not included in the vector X.

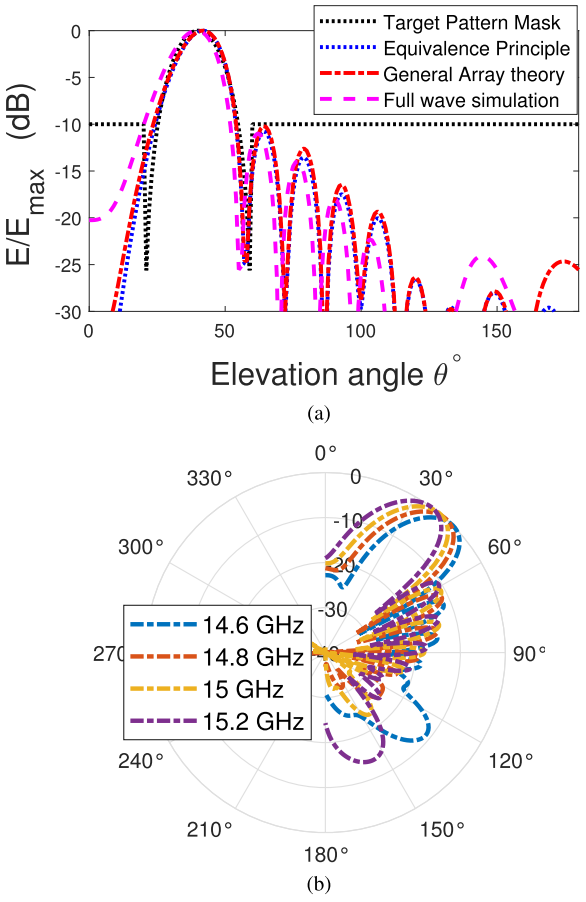

FIGURE 11. Optimized results in elevation plane for design example#2 (a) Normalized radiation pattern at frequency 15 GHz (b) Simulated normalized directivity plots showing frequency scanning behavior.

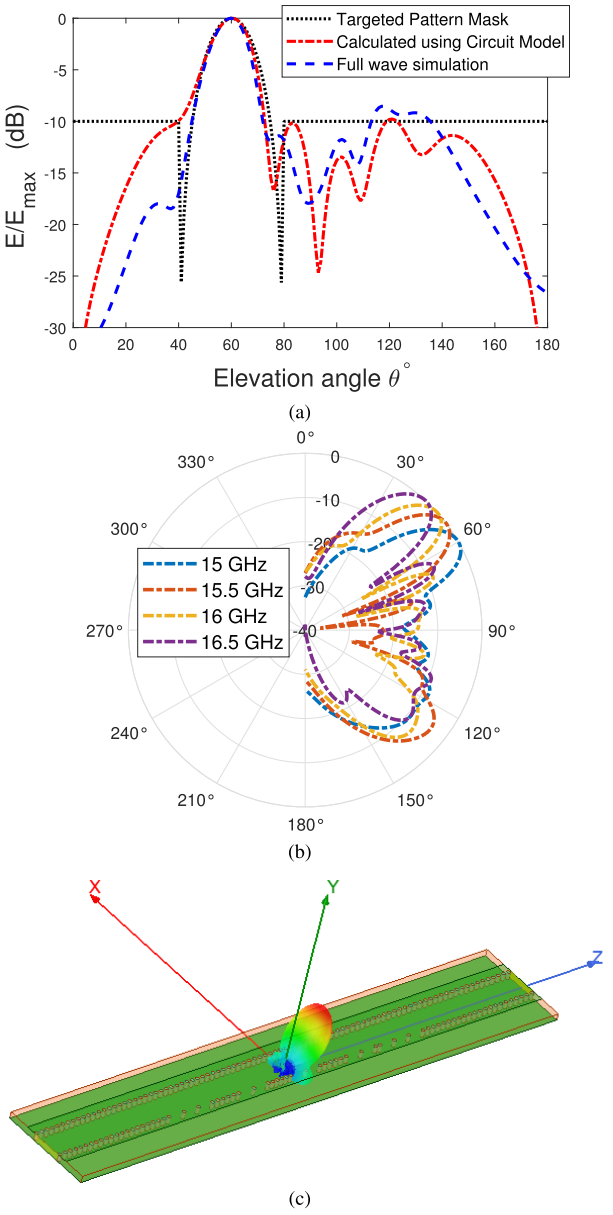

FIGURE 12. Solution#1 plots (a) Normalized radiation pattern in elevation plane at frequency 15 GHz (b) Simulated normalized directivity plots (dB) for showing frequency scanning behavior in the elevation plane (c) Radiating segment of antenna with pattern at 15 GHz.

Varying constraints could result in other possible solutions. The precision of achieving the intended pattern could be influenced by the selection of population and generation sizes in the genetic algorithm. The importance lies in validating the final optimized result through comprehensive full-wave simulation, typically requiring only a single simulation. In most cases, the focus is not on the precise distribution of pattern across all angles. Instead, it is primarily concerned with certain properties of pattern that must meet specific criteria, such as minimizing sidelobes or achieving maximum gain in a specific direction. Therefore, employing a cost function in the optimization process proves to be highly advantageous as it allows to effectively assess and describe performance.

1) DESIGN EXAMPLE # 1

Waveguide dimensions a and b are defined to be 12.5 mm and 1.575 mm respectively for a lossy dielectric Rogers RT/duroid 5880 with $\epsilon_r = 2.2$. Each slot has a length of 3 mm. Extended PEC plane is realized above and below the conductor wall with slots, as in the previous section, to calculate radiation pattern using the equivalence principle as well as general array theory. Using MATLAB, P and n are obtained through optimization of cost function and simulation, with the desired steering angle $\theta_{desired}$ of beam set to 80° and setting $\theta_{FN1} = 65°$, $\theta_{FN2} = 95°$ at 14.5 GHz. For $n = 13$ and $P = [4.01\ 5.83\ 1.02\ 1.86\ 7.56\ 1.01\ 1.31\ 7.98\ 1.15\ 1.19\ 7.42\ 3.28]$ mm, the desired pattern with the desired peak angle and beamwidth is achieved by exciting port1. The results are presented in Fig. 10, with the maximum peak side lobe level (PSLL) found to be −11.6 dB at 14.5 GHz on the full wave simulator. HPBW is 13° here. The full wave simulated result is in good agreement with the calculated patterns using the circuit model, except for some discrepancies in the side lobe region. However, as long as SLL is less than −10 dB, differences in patterns can be neglected.

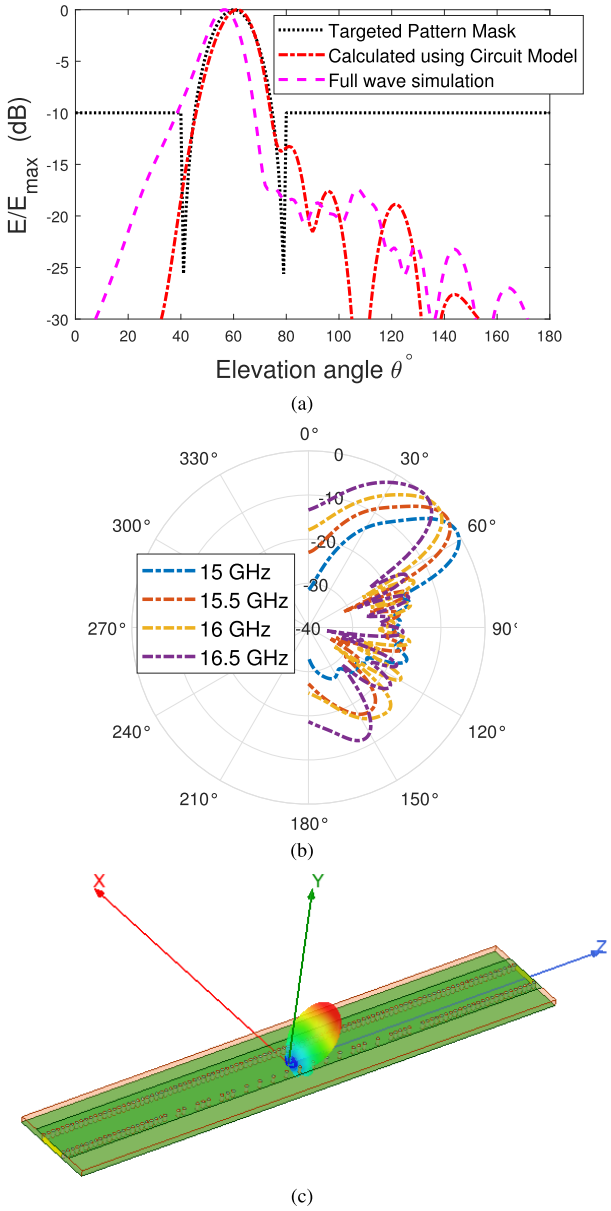

FIGURE 13. Solution#2 plots (a) Normalized radiation pattern in elevation plane at frequency 15 GHz (b) Simulated normalized directivity plots (dB) for showing frequency scanning behavior in the elevation plane (c) Radiating segment of antenna with pattern at 15 GHz.

The intrinsic nature of the leaky wave antenna for steering the beam with a change in frequency without significantly distorting the beam shape can be observed in Fig. 10(b). The beam covers roughly 21° scanning range in the elevation plane for a frequency range of 12.5 GHz - 15.5 GHz, with an average scanning of 6.6° observed for a 1 GHz change in frequency.

2) DESIGN EXAMPLE # 2

The antenna design uses Rogers RT/duroid 5870 as lossy dielectric and $\epsilon_r = 2.33$, with each slot defined to be of length 4 mm. The waveguide dimensions are $a = 7$ mm, $b = 0.508$ mm. The PEC wall is extended around slots as in the previous example. The desired steering angle $\theta_{desired}$ of the beam is set to 40° with the first nulls defined as 20° and 60°, resulting in FNBW of 40° at 15 GHz. The results are presented in Fig. 11, with the PSLL found to be −10.2 dB at 15 GHz on a full wave simulator. The best possible result to get the desired pattern is achieved using $n = 9$, $P = [4.25\ 5.28\ 6.82\ 6.87\ 4.63\ 7.54\ 6.38\ 3.47]$ mm, and by exciting port1. HPBW obtained is 17° as of desired one. The full wave simulated result is in agreement with those for the calculated patterns using the circuit model, except for some anomalies outside the main lobe region. However differences in patterns can be neglected as SLLs are below −10 dB. Also, the shape of sidelobes is not intended, but their levels. The simulated frequency scanning behavior can be observed in Fig. 11(b) for a frequency range of 14.6 GHz - 15.2 GHz without any deterioration in beam shape. An average scanning of 3° is observed for every 200 MHz change in frequency.

V. EXPERIMENTAL VALIDATION

Experimental validation is conducted using an antenna fabricated with Rogers RT/duroid 5880, a lossy dielectric with a relative permittivity of 2.2 and tanδ of 0.0009. The desired steering angle ($\theta_{desired}$) of the beam is set to 60°, with first nulls at 40° and 80°, resulting in a FNBW of 40° at 15 GHz. The selection of 15 GHz is based on its proposal as one of the frequency candidates for 5G mobile communication by NTT DoCoMo and Ericsson [25]. It is motivated by its advantages over higher frequencies, such as 28 GHz and 60 GHz, offering reduced rain attenuation, lower propagation loss, and system simplicity [26]. It has been used for beamforming and 5G radio access [27]. The design of a prototype antenna for urban 5G applications at 15 GHz is also presented in [9], following specifications provided in [3].

S-parameters and element pattern are obtained for unit slot SIW structure, similar to the one in [3]. Admittances are calculated by using (2). Voltages across admittances are obtained using the proposed circuit model for equivalent rectangular waveguide with slots. The antenna design includes slots of length 3 mm, equivalent rectangular waveguide width $a = 7$ mm, and substrate height $b = 1.575$ mm. Populations 50 in each of 100 generations are used in the GA algorithm. SIW is implemented using optimized X and replicating unit slot waveguide structure. The width of the SIW used is the one calculated by using equations given in [16] and [17]. Two possible optimal solutions are achieved for a targeted pattern here.

A. SOLUTION # 1

The optimal design requires n and P to be 12 and [1, 1, 8, 1, 7, 1, 8, 1, 2, 1, 1] mm respectively, when integer optimization is conducted. Considering manufacturer constraints, dia(d) of via chosen is 0.8 mm, and edge-to-edge spacing between vias is not less than 20 mils, resulting in modified P to be [0.8, 0.8, 8, 0.8, 7, 0.8, 8, 0.8, 2, 0.8, 0.8] mm. The simulation results indicate a PSLL of −8.5 dB at 15 GHz.

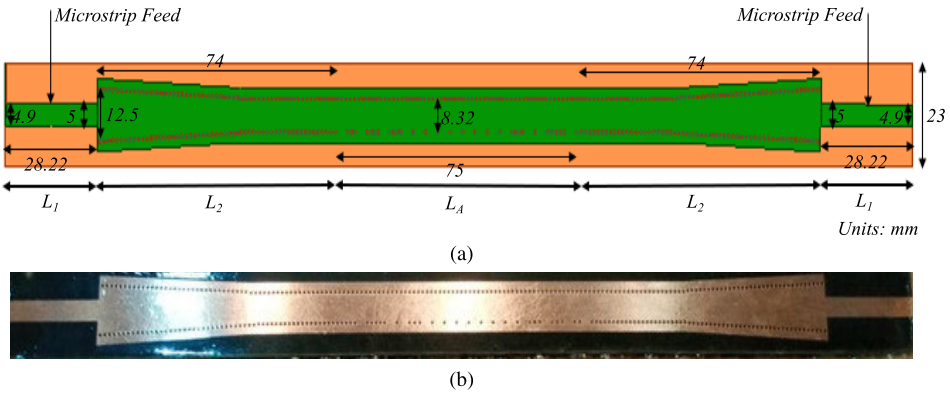

FIGURE 14. Fabricated antenna (a) Antenna along with feed and impedance matching structure: Microstrip feed and transition from microstrip feed to SIW(L_1), SIW to LWA transition(L_2), and radiating LWA(L_A) (b) Photograph of the fabricated SIW LWA (Top view).

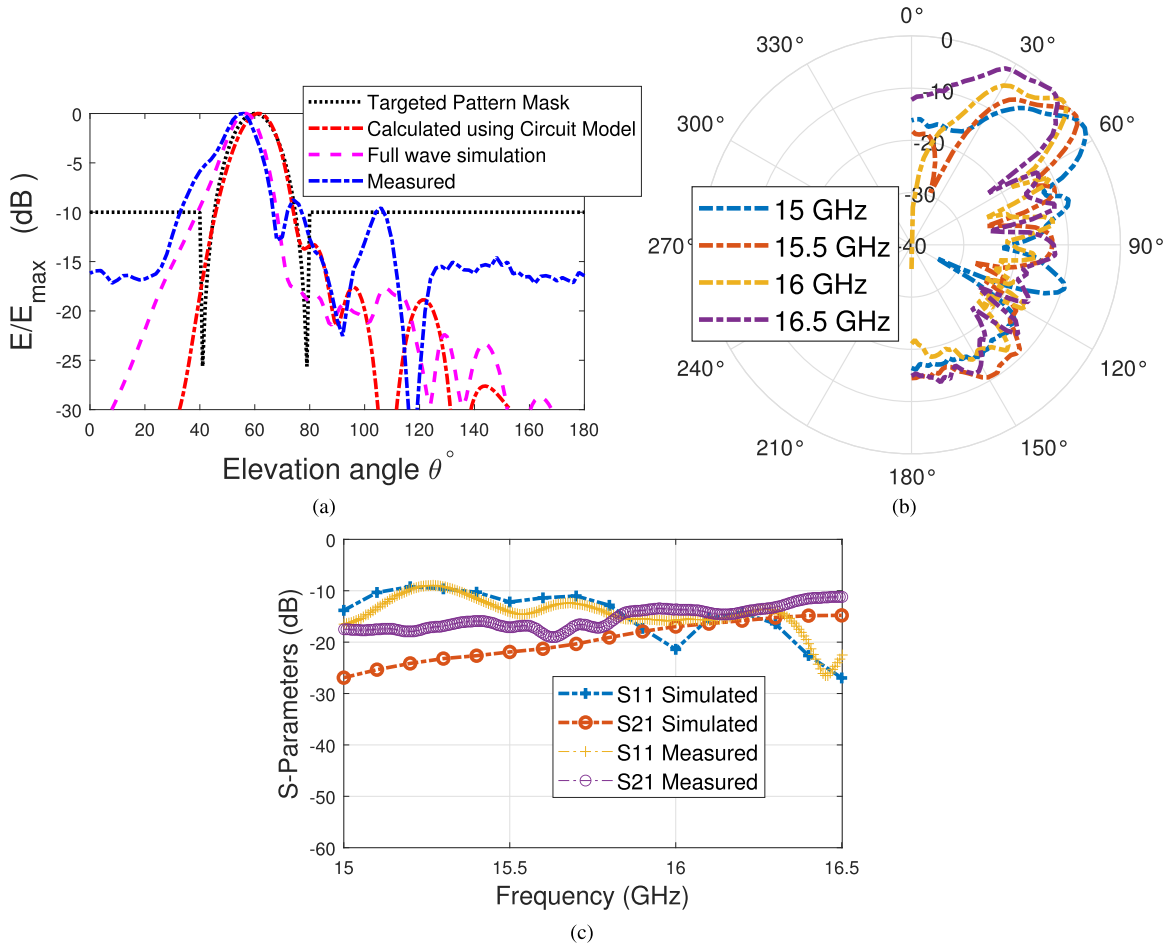

FIGURE 15. Measured results (a) Normalized radiation pattern at 15 GHz in the elevation plane (b) Normalized radiation pattern (dB) scanning with a change in frequency (c) S-parameters.

HPBW of pattern mask is almost 18°, whereas HPBW through full-wave simulation is 15°. Peak is observed to be at $\theta = 60°$ and $\phi = 90°$ in the 3D pattern. Fig. 12 displays the results. Simulated frequency scanning behavior is observed for a frequency range of 15 GHz to 16.5 GHz, with an average scanning of 5° for every 0.5 GHz change in frequency.

B. SOLUTION # 2

The optimal design requires n and P to be 15 and [3, 4, 4, 1, 1, 1, 1, 1, 1, 1, 1, 4, 1, 6] mm respectively. However, due to mechanical constraints, d is 0.8 mm, and edge-to-edge spacing between vias is not less than 20 mils. This results in modified P to be [2.4, 4, 4, 0.8, 0.8, 0.8, 0.8, 0.8, 0.8, 0.8, 0.8, 4, 0.8, 6] in mm. The simulation results indicate a

TABLE 1. Comparison of the proposed model with other models for SIW LWAs.

Ref.	Design Methodology	Cost Function	Leaky Wave Antenna Structure	Performance Evaluation	Novelty
[3]	SIW LWA modeled as TEN with radiation control (adjustments of W and P)	Minimization of the sum of impedances in TEN at the reference plane for an unknown complex leaky mode wavenumber	Periodic structure on one side of SIW LWA achieved by altering distances between vias to enhance energy radiation through Partially Reflecting Surface (PRS) wall	Achieves desired scanning angle (θ_{RAD}) and directivity control by altering W and P at a specific frequency	Precise modeling of metallic posts using T-impedance network and pattern synthesis with independent control of leakage rate and phase constant
[4]	SIW LWA modeled along the axis of propagation, utilizing waveguide circuit theory for accurate aperture field distribution and global optimization based on S-parameters computations	Application-dependent criteria, such as low SLL, large realized gain, wide null, desired scanning angle, and pattern masking	Continuous source LWA with smooth structure variation or periodic structures with closely spaced radiating elements	Focuses on scanning angle, low side lobe level (SLL), realized gain, and null control at the operating frequency through smooth variation in antenna structure	Utilizes waveguide circuit theory and pattern synthesis without the need for separate control of the leakage rate and phase constant along the antenna length
[5]	Array theory: Utilizes frequency-dependent main beam directions for both element pattern and array factor.	Pattern at desired angle = optimized element pattern x array factor with manipulated phase at a specific frequency	Generic LWA structures	Utilizes frequency-sensitive element patterns for expanded scanning, adjusts the main beam via the phase difference of two ports, and ensures stable gain and radiation	Enables wide scanning with changes in frequency and pattern synthesis using a nonconventional array theory approach
[6]	A unique simulation model, incorporating field simulations of single slot elements and a meandered waveguide curve modeled as a transmission line between adjacent slots, tailors the far-field pattern by modifying slot dimensions and associated amplitude weighting coefficients	Maximization of antenna gain for an optimal slot count to balance performance parameters, including antenna efficiency and directivity	Slotted waveguide structure on nonconventional SIW technology	Represents waveguide losses, compensates through amplitude weighting, and strategically adjusts slot dimensions to achieve weightings that reduce sidelobe levels in the radiation pattern	Compensates for waveguide losses and pattern synthesis by adjusting slot dimensions and associated weights
This work	Antenna modeled as a circuit along the axis of propagation, with slots represented as admittances for pattern synthesis	Pattern matching to minimize the difference between targeted and calculated patterns. It can be based on any application-dependent criteria	Quasi-periodic or even periodic structure on one side achieved by increasing via distances for effective radiation	Optimizes for desired scanning angle, beamwidth, and SLL by changing the number of slots, spacing between them, and opening of slots at a specific frequency	Pattern synthesis and optimization for quasi-periodic and periodic structures using equivalent circuit models. Real and imaginary parts of the admittances for the slots contribute to both leakage effects and phase variations along the antenna length.

PSLL of -17.55 dB at 15 GHz. HPBW of the desired shape is 18°, whereas HPBW through full-wave simulation is 14°. The peak of the 3D pattern is observed to be at $\theta = 57°$ and $\phi = 97°$. Fig. 13 displays the simulated frequency scanning behavior for a frequency range of 15 GHz to 16.5 GHz, with an average scanning of 5° observed for every 0.5 GHz change in frequency.

The optimization tasks have been conducted on a computing system equipped with an 11th Gen. Intel Core i5-1135G7 processor, operating at 2.40 GHz and utilizing an x64-based architecture. The system is equipped with 16 GB of RAM. The comparative analysis focused on the time per iteration for full-wave simulation and for genetic algorithm-based optimization using the proposed circuit model across varying slot numbers and spacing between slots. The maximum number of slots used for optimization is 40. In MATLAB, the proposed method has indicated an average simulation time of ∼4 seconds per iteration, whereas simulations conducted on a full-wave simulator like High Frequency Structure Simulator (HFSS) have shown a substantial increase, with an average simulation time of 4 minutes and 55 seconds per iteration. Increasing the generation size can further extend the completion time for the optimization task, especially when employing the full-wave simulation approach. Clearly,

increasing the number of iterations to 200 or 300 could intensify the computational burden, making it a highly time-consuming task in the context of full-wave simulation.

The second solution has been manufactured with a focus on achieving low side lobe levels (SLLs). Also, S-parameters are found to be good for solution#2 and below −10 dB as compared to those of solution#1 for the whole frequency range.

The feed can be connected to a planar waveguide structure through a microstrip line on the same dielectric substrate [28]. Equations provided in [29] are utilized to design a microstrip to SIW transition that offers complete bandwidth coverage without requiring optimization. To enhance radiation efficiency, the dielectric material is extended beyond vias as in [3]. Fig. 14 illustrates the antenna that has been fabricated.

In Fig. 15(a), the measured radiation pattern is compared to simulations in the elevation plane. The target peak is 60° with a 18° HPBW. However, the calculated pattern peaks at 61° with a 13° HPBW. Full wave simulation shows a peak at 57° with a 14° HPBW and measured data show a peak at 56° with a 13° HPBW. These variations can be due to imperfect metallic surface coverage during testing. However, a good approximation is achieved in the main beam area of the pattern, where radiation is primarily due to leaky waves. To explore beam steering, radiation patterns at different frequencies are tested, as depicted in Fig. 15(b). A quick analysis reveals that the measured patterns exhibit higher side lobe levels compared to the simulated ones in Fig. 13. This discrepancy can be attributed to partial coverage of metallic surfaces during testing, diffraction effects from finite ground plane, and excitation of surface waves. Fig. 15(c) presents the S-parameters. Although $|S_{11}|$ values occasionally reach −9 dB at specific frequencies, overall matching performance remains acceptable. Considering both radiation and reflection effects, what remains is the power reaching port 2, indicated here by $|S_{21}|$ values. Port 2 serves as the output port terminated with a matched load. Notably, the $|S_{21}|$ parameter consistently stays below -10 dB across the frequency range, emphasizing substantial energy leakage from the antenna, while reflection is already minimal. However, a discrepancy in the level of $|S_{21}|$ between simulation and measurement is noted. This difference might arise from fabrication errors, metallization of vias, etc.

The characteristics of the proposed TL model are compared to those of other models in the Table 1.

VI. CONCLUSION

The research introduces a novel and efficient approach for designing substrate-integrated waveguide leaky wave antennas. Utilizing a generic circuit model, this method enables accurate radiation pattern synthesis in both periodic and quasi-periodic structures, offering faster analysis compared to the conventional method of full-wave simulation, while maintaining reasonable accuracy. The versatility of this technique in controlling side lobe levels and achieving desired beam shapes through optimization algorithms makes it a valuable tool for practical antenna designs. The antenna can be optimized for various possible radiation patterns by choosing an application-specific cost function. With its contributions to enhancing antenna engineering capabilities, this work paves the way for further innovations in SIW-based antenna design for future wireless communication systems and 5G applications.

ACKNOWLEDGMENT

The authors would like to thank Rogers Corporation for providing PCB sheets, to Bismillah Electronics, Lahore, Pakistan, and ElitePCB, Karachi, Pakistan, for the facilitation of antenna fabrication, and to NUST RIMMS, Pakistan, for measurements. Their contributions were vital to the successful completion of this project.

REFERENCES

[1] D. Deslandes and K. Wu, "The substrate integrated waveguide (SIW)—Concept, technology and applications," in *Proc. 10th Int. Symp. Microwave Opt. Technol. (ISMOT)*, Fukuoka, Japan, Aug. 2005, pp. 598–601.

[2] D. Zheng, C. H. Chan, and K. Wu, "Leaky-wave structures and techniques for integrated front-end antenna systems," *IEEE J. Microwave*, vol. 3, no. 1, pp. 368–397, Jan. 2023.

[3] A. J. Martinez-Ros, J. L. Gómez-Tornero, and F. Quesada-Pereira, "Efficient analysis and design of novel SIW leaky-wave antenna," *IEEE Antennas Wireless Propag. Lett.*, vol. 12, pp. 496–499, 2013.

[4] N. Nguyen-Trong, L. Hall, and C. Fumeaux, "Transmission-line model of nonuniform leaky-wave antennas," *IEEE Trans. Antennas Propag.*, vol. 64, no. 3, pp. 883–893, Mar. 2016.

[5] W.-H. Li, B. Wu, H.-R. Zu, T. Su, and Y.-F. Fan, "Design of leaky wave antenna with wide angle backfire to forward beam scanning based on generalized pattern synthesis," *IEEE Trans. Circuits Syst. II Exp. Briefs*, vol. 70, no. 7, pp. 2625–2629, Jul. 2023.

[6] P. Kwiatkowski, A. Orth, and N. Pohl, "A novel simulation model for design of frequency steered slotted waveguide antennas in SIW technology for accurate far field synthesis," in *Proc. German Microwave Conf.*, Cottbus, Germany, Mar. 2020, pp. 48–51.

[7] N. Bayat-Makou, K. Wu, and A. A. Kishk, "Single-layer substrate-integrated broadside leaky long-slot array antennas with embedded reflectors for 5G systems," *IEEE Trans. Antennas Propag.*, vol. 67, no. 12, pp. 7331–7339, Dec. 2019.

[8] Y.-L. Lyu, X.-X. Liu, P.-Y. Wang, D. Erni, Q. Wu, C. Wang, N.-Y. Kim, and F.-Y. Meng, "Leaky-wave antennas based on noncutoff substrate integrated waveguide supporting beam scanning from backward to forward," *IEEE Trans. Antennas Propag.*, vol. 64, no. 6, pp. 2155–2164, Jun. 2016.

[9] F. M. Monavar, S. Shamsinejad, R. Mirzavand, J. Melzer, and P. Mousavi, "Beam-steering SIW leaky-wave subarray with flat-topped footprint for 5G applications," *IEEE Trans. Antennas Propag.*, vol. 65, no. 3, pp. 1108–1120, Mar. 2017.

[10] L. Goldstone and A. Oliner, "Leaky-wave antennas I: Rectangular waveguides," *IEEE Trans. Antennas Propag.*, vol. 7, no. 4, pp. 307–319, Oct. 1959.

[11] R. S. Elliott, "Radiation patterns of horns, slots and patch antennas," in *Antenna Theory & Design*, Revised Ed. Hoboken, NJ, USA: Wiley, 2003, ch. 3, pp. 91–99.

[12] T. Vaupel, "A MFIE/EFIE fast multipole volume/surface integral equation approach for substrate integrated waveguide structures and leaky-Wave/Slot antennas using the duality principle," in *Proc. Int. Conf. Electromagn. Adv. Appl. (ICEAA)*, Granada, Spain, Sep. 2019, pp. 0373–0377.

[13] M. Casaletti, G. Valerio, J. Seljan, M. Ettorre, and R. Sauleau, "A full-wave hybrid method for the analysis of multilayered SIW-based antennas," *IEEE Trans. Antennas Propag.*, vol. 61, no. 11, pp. 5575–5588, Nov. 2013.

[14] D. Zheng and K. Wu, "Radiating discontinuity in leaky-wave antenna: A role in complex propagation constant engineering," in *Proc. IEEE Int. Symp. Antennas Propag. North Amer. Radio Sci. Meeting*, Montreal, QC, Canada, Jul. 2020, pp. 417–418.

[15] D. Deslandes and K. Wu, "Accurate modeling, wave mechanisms, and design considerations of a substrate integrated waveguide," *IEEE Trans. Microwave Theory Techn.*, vol. 54, no. 6, pp. 2516–2526, Jun. 2006.
[16] D. Deslandes and K. Wu, "Design consideration and performance analysis of substrate integrated waveguide components," in *Proc. 32nd Eur. Microwave Conf.*, Milan, Italy, Sep. 2002, pp. 1–4.
[17] F. Xu and K. Wu, "Guided-wave and leakage characteristics of substrate integrated waveguide," *IEEE Trans. Microwave Theory Techn.*, vol. 53, no. 1, pp. 66–73, Jan. 2005.
[18] D. Deslandes and K. Wu, "Substrate integrated waveguide leaky-wave antenna: Concept and design considerations," in *Asia–Pacific Microwave Conf. Proc.*, Suzhou, China, 2005, pp. 346–349.
[19] N. Nguyen-Trong, T. Kaufmann, and C. Fumeaux, "A semi-analytical solution of a tapered half-mode substrate-integrated waveguide with application to rapid antenna optimization," *IEEE Trans. Antennas Propag.*, vol. 62, no. 6, pp. 3189–3200, Jun. 2014.
[20] N. Nguyen-Trong, L. T. Hall, and C. Fumeaux, "Pattern synthesis with angular mask for leaky-wave antennas," in *Proc. 17th Int. Symp. Antenna Technol. Appl. Electromagn. (ANTEM)*, Montreal, QC, Canada, Jul. 2016, pp. 1–2.
[21] N. Nguyen-Trong, T. Kaufmann, L. Hall, and C. Fumeaux, "Optimization of leaky-wave antennas based on non-uniform HMSIW," in *Proc. IEEE MTT-S Int. Conf. Numer. Electromagn. Multiphys. Optim. (NEMO)*, Ottawa, ON, Canada, Aug. 2015, pp. 1–4.
[22] E. Liu, J. Geng, K. Wang, H. Zhou, C. Reng, J. Zhang, X. Zhao, X. Liang, and R. Jin, "Generalized principle of pattern multiplication based on the phase antenna element," in *Proc. IEEE Int. Symp. Antennas Propag. North Amer. Radio Sci. Meeting*, Montreal, QC, Canada, Jul. 2020, pp. 353–354.
[23] D. M. Pozar, "Microwave network analysis," in *Microwave Engineering*, 4th ed. Hoboken, NJ, USA: Wiley, 2012, pp. 188–194.
[24] C. A. Balanis, "Arrays: Linear, planar, and circular," in *Antenna Theory: Analysis and Design*, 3rd ed. Hoboken, NJ, USA: Wiley, 2005, pp. 283–290.
[25] K. Tateishi, D. Kunta, A. Harada, Y. Kishryama, S. Parkvall, E. Dahlman, and J. Furuskog, "Field experiments on 5G radio access using 15-GHz band in outdoor small cell environment," in *Proc. IEEE 26th Annu. Int. Symp. Pers., Indoor, Mobile Radio Commun. (PIMRC)*, Hong Kong, Aug. 2015, pp. 851–855.
[26] W.-C. Cheng, T.-H. Liu, M.-L. Hsu, Z.-M. Tsai, and W.-H. Sheen, "15 GHz propagation channel measurement at a University campus for the 5G spectrum," in *Proc. Asia–Pacific Microwave Conf. (APMC)*, vol. 2, Nanjing, China, Dec. 2015, pp. 1–3.
[27] D. Kurita, K. Tateishi, A. Harada, Y. Kishiyama, S. Itoh, H. Murai, A. Simonsson, and P. Okvist, "Indoor and outdoor experiments on 5G radio access using distributed MIMO and beamforming in 15 GHz frequency band," in *Proc. IEEE Globecom Workshops*, Washington, DC, USA, Dec. 2016, pp. 1–6.
[28] D. Deslandes and K. Wu, "Integrated microstrip and rectangular waveguide in planar form," *IEEE Microwave Wireless Compon. Lett.*, vol. 11, no. 2, pp. 68–70, Feb. 2001.
[29] D. Deslandes, "Design equations for tapered microstrip-to-Substrate integrated waveguide transitions," in *IEEE MTT-S Int. Microwave Symp. Dig.*, Anaheim, USA, May 2010, pp. 704–707.

NASIM ZAHRA received the B.Sc. degree in electrical engineering and the M.Sc. degree in electrical engineering (electronics and telecommunication) from the University of Engineering and Technology Lahore (UET Lahore), Lahore, Pakistan, in 2007 and 2013, respectively, where she is currently pursuing the Ph.D. degree in electrical engineering. Her research interests include antenna theory and design, array signal processing, reconfigurable antennas, electromagnetics, and electromagnetic compatibility.

FAROOQ MUKHTAR received his B.Sc. degree in Electrical Engineering from the University of Engineering and Technology (U.E.T), Lahore, Pakistan, in 2007 and started his career as a tutor for high-frequency courses and as a Lab-Engineer for electromagnetic compatibility (EMC) testing at the same university. He then earned an M.Sc. in Microwave Engineering and a Dr.-Ing. degree under Prof. Peter Russer from the Technical University Munich, Germany, in 2009 and 2014. During that time, he worked as a part-time scientific co-worker at the Institute for Nanoelectronics on algorithms for Brune's synthesis of multiport circuits and conducted tutorials on the post-graduate course "Quantum Nanoelectronics." Currently, he is an Assistant Professor with UET Lahore, working on high-frequency topics: leaky wave and configurable antennas, filters, and metamaterials. He is also consulting Smart Wires Inc., through Powersoft19 in the areas of electromagnetic simulations and compatibility.

INAM ELAHI RANA received his B.Sc. degree in Electrical Engineering from U.E.T, Lahore, in 1974, and joined Suparco. After receiving a scholarship from Suparco, he joined UCLA and earned M.S. and Ph.D. degrees in 1977 and 1979, respectively. Having had a mixed career in both industry and academia, he has been involved in the design and development of several projects for different organizations. He has taught various courses in electromagnetics, antennas, electromagnetic compatibility, and microwave engineering at different universities, both at undergraduate and graduate levels. Currently, he is the CEO of Bismillah Electronics Lahore.

MAHRUKH KHAN received the Bachelor of Science and Master of Science degrees in electrical engineering from the University of Engineering and Technology, Lahore, Pakistan, in 2007 and 2011, respectively, and the Ph.D. degree in electrical engineering from the University of Missouri-Kansas City, Kansas City, MO, USA, in 2017.

Prior to joining TCNJ as an Assistant Professor, she was an Assistant Research Professor with Missouri Institute of Defense and Energy (MIDE), University of Missouri-Kansas City (UMKC), where she was a Postdoctoral Fellow with the Micro and Nano-Technology Laboratory, Computer Science and Electrical Engineering Department (CSEE), from January 2018 to December 2019. She is currently an Assistant Professor with The College of New Jersey (TCNJ), NJ, USA. She is also the Co-Director of the Microwave and Wireless Communication Laboratory (MWCL), TCNJ. She has published more than 30 articles and conference papers in renowned journals and peer-reviewed conferences in her field of research. Her research articles and conference papers have received more than 250 citations in a short period.

Dr. Khan is a Senior Member of URSI and an active member of IEEE Young Professionals and IEEE Women in Engineering Societies. She was selected as a 2022 IEEE Antennas and Propagation (APS) Young Professional Ambassador. She won an honorable mention in the international 2015 Altair FEKO Student Competition and the Prestigious UMKC School of Graduate Studies (SGS) Fellowship for her outstanding research. She has served as a Reviewer for top-notch peer-reviewed journals, such as *IEEE Antennas and Propagation Magazine* and *IET Microwaves, Antennas & Propagation*.